Evaluation of optical multi-spectral satellite data for crop type and land cover identification in Marathwada, India: a disaster management perspective

Kale Shashikant Rangnathrao*, Holambe Raghunath Sambhaji and Chile Rajan Hari
[1]Department of Instrumentation Engineering, SGGS Institute of Engineering and Technology, Vishnupuri, Nanded, INDIA
*shashikantkale87@gmail.com

Abstract
This study evaluates the use of optical multi-spectral satellite data for crop type and land cover identification in Marathwada, India, with a specific focus on disaster management. The region is highly susceptible to various disasters including droughts and other climate-related events that significantly impact agricultural productivity. The study involves analyzing both single-date and multi-temporal satellite imagery to develop composite images using different band combinations, aiming to identify the most accurate combination for crop and land cover identification. A multi-class classification approach based on random forest is employed for feature extraction and the significance of different bands in the imagery is assessed.

The results demonstrate that a composite image composed of Red, Green, Blue, Near Infrared and Shortwave Infrared bands yields the highest accuracy with an overall accuracy (OA) of up to 93.69% for all land cover classes and 91.18% for crop classes alone, using six-date multi-temporal imagery. The findings highlight the potential of optical multi-spectral satellite data as an effective tool for crop type and land cover identification in Marathwada, India, particularly in the context of disaster i.e. agricultural draught management. The methodologies and results presented in this study can serve as a valuable reference for similar research endeavors in other agricultural draught prone regions of India and beyond.

Keywords: Crop identification, Land cover identification, Disaster management, Remote sensing, Random Forest (RF) classifier, Satellite image analysis.

Introduction

Agriculture serves as a vital source of direct or indirect income for more than two-thirds of the population in Maharashtra state[14,24] and plays a crucial role in the Indian economy. However, the agricultural sector faces numerous challenges including the increasing frequency of disasters such as droughts caused by low rainfall[1]. India, being one of the most vulnerable and drought-prone countries globally, has experienced recurrent drought conditions over the past few decades[15,24]. In response, the Government has implemented various schemes to support farmers and their families.[4,6]

Drought is a prolonged period of abnormally low rainfall which can have severe impacts on agricultural productivity and the overall ecosystem.[7] It is considered one of the most significant agricultural disasters worldwide. Drought significantly affects crop production by limiting the availability of water, which is crucial for plant growth and development.[19] Lack of rainfall leads to soil moisture deficits, resulting in water stress for crops. This water stress negatively impacts the physiological processes of plants such as photosynthesis, nutrient uptake and root development. Consequently, crop yields can be drastically reduced or even lead to crop failure.[22]

Accurate identification of drought-affected regions and timely support are crucial for effective disaster management in agriculture. Manual surveys with their inherent limitations such as time consumption, potential misstatements and forgetfulness, often result in inaccurate records. Satellite image analysis has emerged as a valuable tool in various geographic applications including agricultural monitoring.[2,5,10,11,13,20,21,25] This study focuses on utilizing satellite imagery analysis to identify major regional crops and other land covers in the Marathwada region of Maharashtra State, India, with a specific emphasis on enhancing agricultural draught management practices.

Accurate crop identification with exceptional precision is a critical aspect of agricultural monitoring[25]. This research aims to improve the accuracy of crop identification by exploring various band combinations of optical imagery with high spatial, spectral and temporal resolution. Additionally, this study seeks to facilitate proper field mapping and precise crop-wise acreage estimation, providing indispensable tools for farmers.[5]

Machine learning classification techniques have been extensively studied for satellite image segmentation. While maximum likelihood (ML) and support vector machine (SVM) algorithms have gained significant attention in remote sensing applications,[8,16,25] the random forest (RF) algorithm has also demonstrated remarkable outcomes in land use and land cover (LULC) applications using remote sensing data.[2,8,16,18] Furthermore, researchers have explored the use of neural network (NN) and convolutional neural network (CNN) for image classification.[11,17] Despite their high accuracy, SVM and CNN algorithms are resource-intensive and require a substantial number of training samples.[11] Various optical and synthetic aperture radar (SAR) data such as Landsat, SPOT 5, Sentinel-2, Indian Remote Sensing (IRS), Radarsat and Sentinel-1, have been

https://doi.org/10.25303/1612da042054

employed for different agricultural applications including crop identification.[9,10,20,23]

The use of optical multi-spectral satellite data for crop type and land cover identification, as explored in this study, holds significant promise for disaster management in the agricultural sector. Accurate identification of crop types and land covers through satellite imagery analysis can provide crucial information for assessing the impact of disasters such as droughts, floods, or storms on agricultural regions. This information enables timely and targeted interventions including resource allocation, relief measures and recovery planning to mitigate the adverse effects of disasters on farmers and their livelihoods.

By leveraging classification techniques like the random forest algorithm and employing moderate-resolution satellite imagery, this research contributes to the development of a robust agricultural monitoring tool that can support effective disaster management practices. The findings and methods presented in this study offer valuable insights for policymakers, agricultural authorities and disaster management agencies, enabling them to make informed decisions and take proactive measures to reduce the vulnerability of agricultural systems to disasters in Marathwada, India and potentially in other regions facing similar challenges globally.

Material and Methods

Study Area and Land Cover Reference Data: The chosen study area is situated in the vast expanse of the Marathwada region in Maharashtra state, India, as depicted in figure 1. The study encompasses a sprawling land area of approximately 2,771 square kilometers. The topography of this region is extremely varied, comprising a range of diverse land features such as agricultural land, cities, villages, rivers, bare land and so forth. Furthermore, agriculture dominates the landscape of this region, playing a crucial role in the economic well-being of its inhabitants.

To obtain accurate ground truth information, we conducted physical visits to various small sites distributed across the selected study region. Each site was given a unique name based on the village or region where it was located and its details are presented in table 1. The collected ground truth reference land cover data was then randomly divided into training and testing subsets to facilitate the implementation of a supervised classification algorithm with high accuracy.

Image Acquisition: To gather the necessary data for this study, satellite images of Sentinel-2 and Landsat-8 optical satellites were obtained during the Rabbi season between December 2017 and January 2018, with spatial resolutions of 10m and 30m respectively. The Sentinel-2 data was procured from the European Space Agency (ESA) while Landsat-8 imagery was acquired from the U.S. Geological Survey (USGS).

The collected data was free of clouds and underwent both radiometric and geometric corrections. Table 2 provides further details regarding the captured dates of the imagery utilized in this study.

Table 1
Details of the Various Sites used for Reference Land Cover Data in Selected Region

S.N.	Field No.	Field Name	Area in Acres
1	2	Erandeshwar	19.03
2	3	Barasgaon	8.40
3	4	Limbgaon	26.71
4	8	Sonkhed	6.91
5	9	Vishnupuri	23.40
6	10	Wadi Muktaji	14.04
7	12	Vishnupuri new	20.58
8	15	Yelgaon Ardhapur	3.66
9	102	AK Sambhaji	7.61
10	201	Limbgaon2	35.11
11	202	Pimpala Lokhande	60.47
12	203	Pimpala Lokhande	132.40
Total			358.32

Table 2
Imagery Captured Dates from the Satellites Used for the Work

Month and Year	Landsat-8	Sentinel-2
December 2017	-	18, 28
January 2018	12	7, 17, 22,27

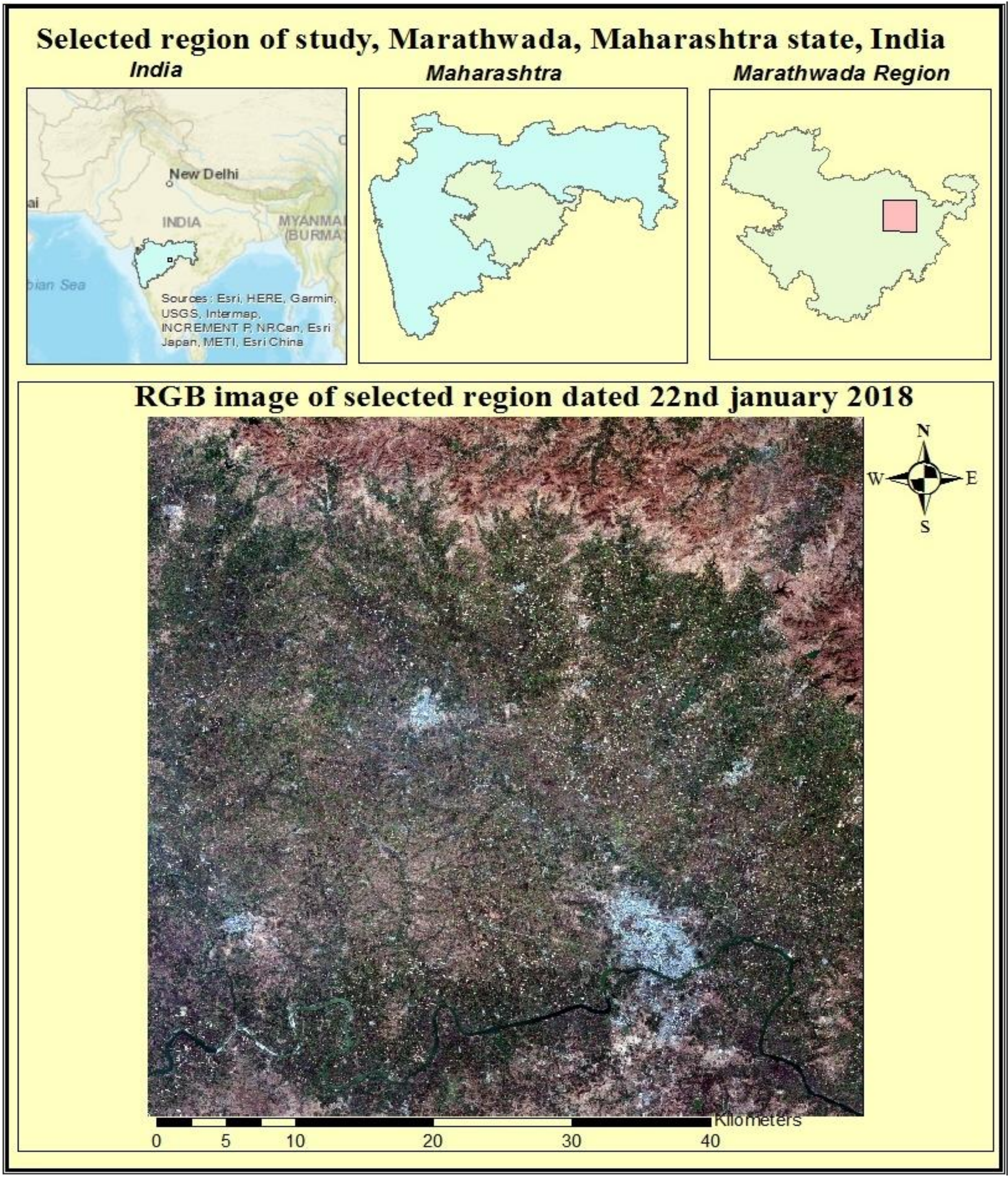

Figure 1: Sentinel-2 Composite RGB Image of Selected Study Region Dated 22nd January 2018

In light of the land cover and agricultural patterns observed in the study area, we have meticulously curated 10 distinct classes as outlined in table 3.

Additionally, the table provides insight into the allocation of training and testing data. The testing phase, aimed at evaluating the model's classification accuracy, was carried out on image pixels covering the aforementioned test sites.

Spectral Reflectance Curve: In order to select the optimal band combination, it is crucial to have a thorough understanding of the reflectance behavior of each band across different classes. This information can be obtained through spectral reflectance curves (SRCs) which reveal the reflectance values of each band for different types of land cover across the electromagnetic spectrum.[12]

Sentinel-2 and Landsat-8, both multi-spectral optical imaging satellites, possess 13 and 11 bands respectively. A few spectral bands are common to both satellites such as Coastal aerosol (C/A), Blue (B), Green (G), Red (R), Near Infrared (NIR), Shortwave Infrared-1 (SWIR1) and Shortwave Infrared-2 (SWIR2).[3] The paired bands exhibit closely aligned central wavelengths. Therefore, spectral reflectance curve (SRC) analysis for the defined classes and required bands is performed using the initial seven bands of Landsat-8 imagery from January 12th, 2018 as demonstrated in table 4.

We have adopted the procedures outlined by Kale and Holambe[8] for the enhancement of land use land cover (LULC) identification through the use of various existing and novel band arithmetic approaches. The development of spectral reflectance curve involved a series of steps as explained in the aforementioned study. Specifically, the spectral reflectance value (L_α) was obtained using the following formula:

$$L_\alpha = \frac{M*DN+\beta}{sin(\theta)} \tag{1}$$

The mathematical formulation involves the calculation of spectral reflectance value (L_α) which is determined by several parameters such as M (Gain value of the band), DN(the gray-scale value of the pixel, also known as Digital number), β(Bias value of the band) and θ (Sun elevation angle). It is noteworthy that the values of M, β and θ are not constant, but instead vary across different satellite images and are documented in the metadata file accompanying the respective satellite data.

The pixel level of the selected area is applied to the Landsat-8 satellite imagery dated January 12, 2018, resulting in the production of reflectance images (one for each band of the satellite imagery). To determine the reflectance value of each class and band, training reference data is utilized.

It is observed that the pixel values for a class exhibit a wide range of variation in these reflectance images. Therefore, mean reflectance values for each class for each band are used which are subsequently transformed into percentage reflectance values to normalize all reflectance values. Reflectance is converted to percentage reflectance ($\%L_\alpha$) for each class in each band using the following formula:

$$\%L_\alpha = \frac{(\mu - R_{min})}{(R_{max} - R_{min})} * 100 \tag{2}$$

where µ is a mean pixel value of the reflectance image of a class calculated from the training data, R_{min} and R_{max} are minimum and maximum of DN values of the reflectance image respectively.

Table 3
Details of Reference Data (Training and Testing) from Various Sites

Class No.	Class Name	Training Area	No. of Test Pixels
1	Sugarcane	8.352	65
2	Chickpea	4.547	40
3	Jowar	1.334	15
4	Wheat	3.558	20
5	Sweet Lime	16.976	150
6	Orange	107.515	450
7	Other Vegetation	11.293	65
8	Bare Land	183.747	140
9	Built-Up Area	9.612	110
10	Water	59.157	260
Total		**406.092**	**1315**

Table 4
Analogous Bands in Sentinel-2 and Landsat-8 Satellite Imagery

S.N.	Name of the band.	Sentinel-2 Band No.	Landsat-8 Band No.
1	Coastal aerosol (C/A)	Band_1	B_1
2	Blue (B)	Band_2	B_2
3	Green (G)	Band_3	B_3
4	Red (R)	Band_4	B_4
5	Near Infrared (NIR)	Band_8	B_5
6	Shortwave Infrared 1 (SWIR1)	Band_11	B_6
7	Shortwave Infrared 2 (SWIR2)	Band_12	B_7

The transformation of reflectance to percentage reflectance values involves the calculation of the mean pixel value (μ) of the reflectance image of a class obtained from the training data. To normalize the reflectance values, the minimum (R_{min}) and maximum (R_{max}) of the DN values of the reflectance image are also determined.

Image Processing: As illustrated in figure 2, the raw Sentinel-2 images undergo a meticulous processing pipeline. In the first stage, the bands with a spatial resolution of 20m or 60m are re-sampled to 10m using the bi-linear interpolation technique. Radiometric corrections are applied to the imagery using the formula and SCP plug-in in the QGIS software. These radiometrically corrected images are then utilized for further processing such as the formation of composite images with various bands on the same date and multi-temporal images. The classifier random forest (RF) is preferred over maximum likelihood (ML) and support vector machine (SVM) after a thorough investigation of its capabilities for the research work. The appropriate bands and composite images with various band combinations were studied through comparison.

The formula is employed to compute the percent reflectance values for all classes for the first seven bands. These values are plotted against the central wavelengths (in meters) of each band as shown in figure 3. The resultant reflectance curves are presented in figures 3 and 4. All the subsequent experiments are conducted using data from the Sentinel-2 satellite, which provides a spatial resolution of 10 meters.

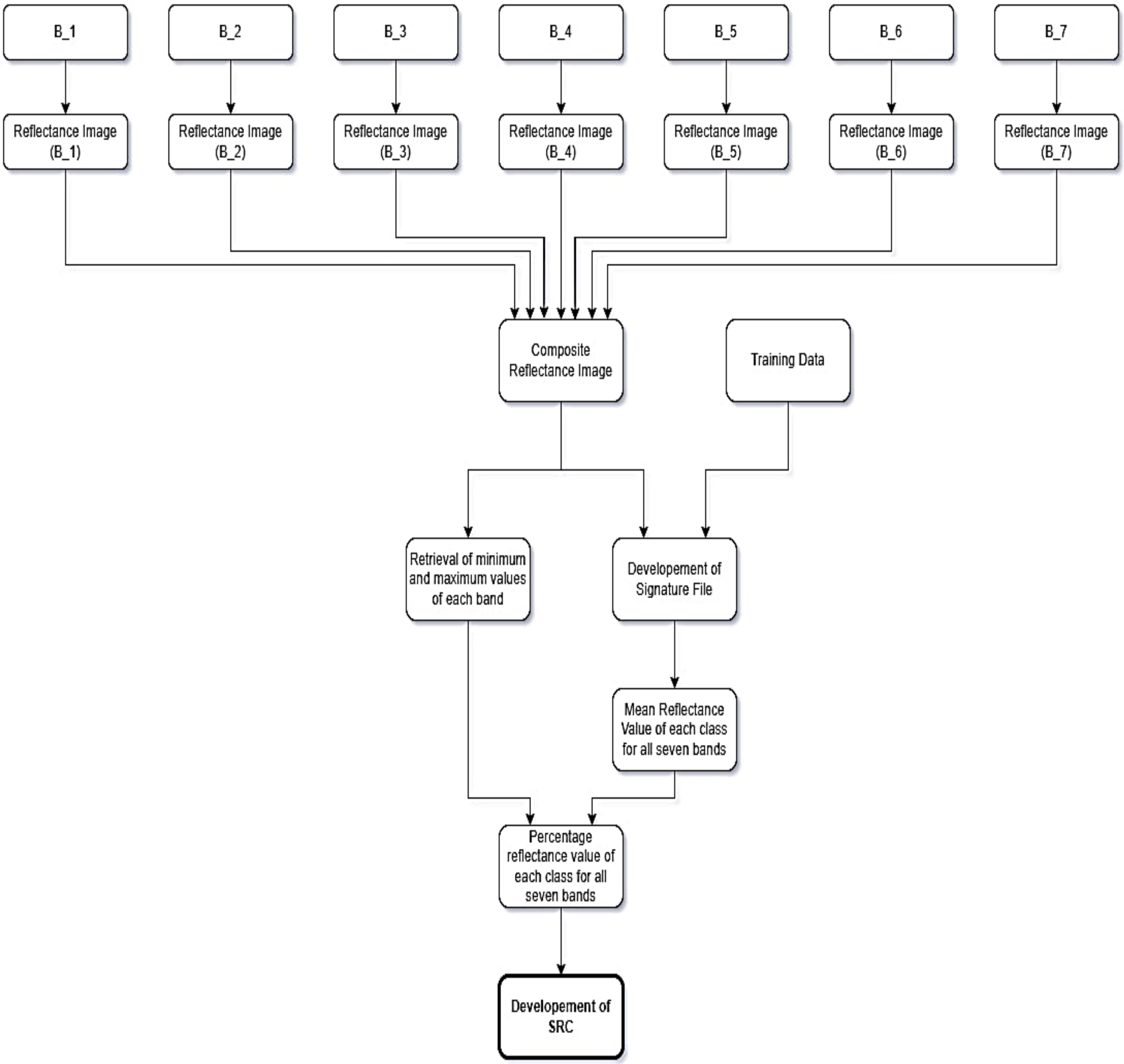

Figure 2: Spectral Reflectance Curve Development Process

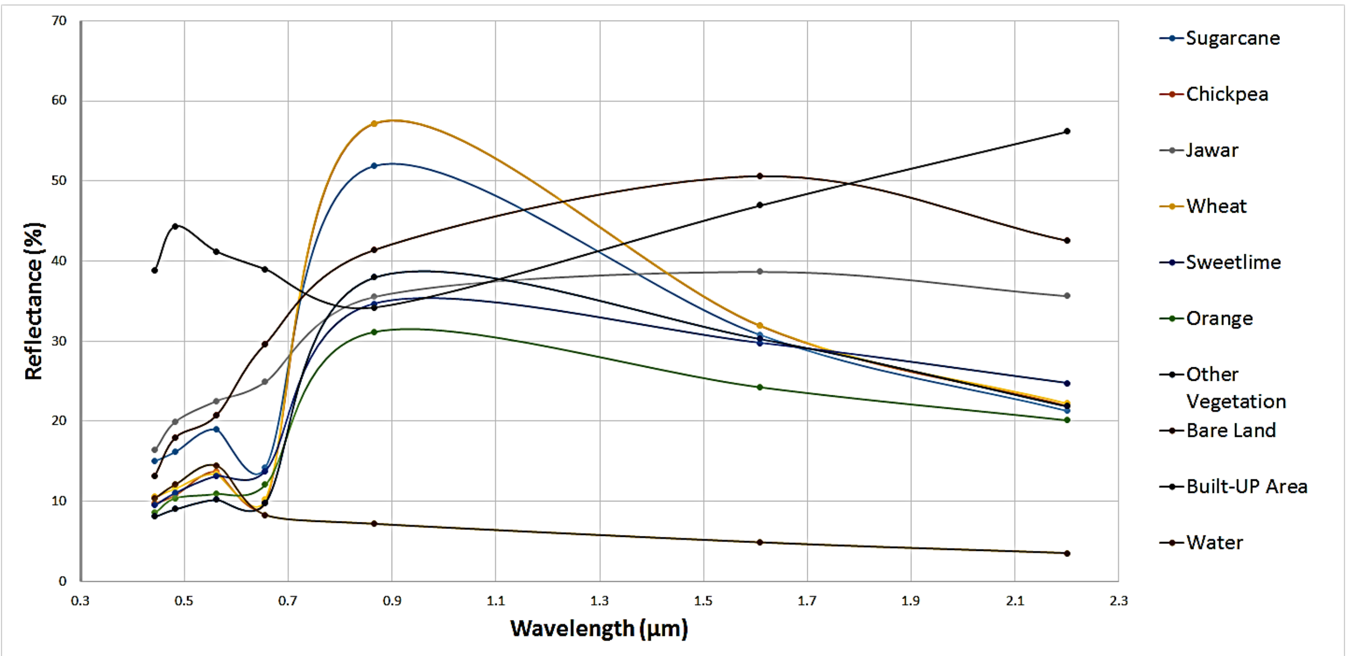

Figure 3: Spectral Reflectance Curve

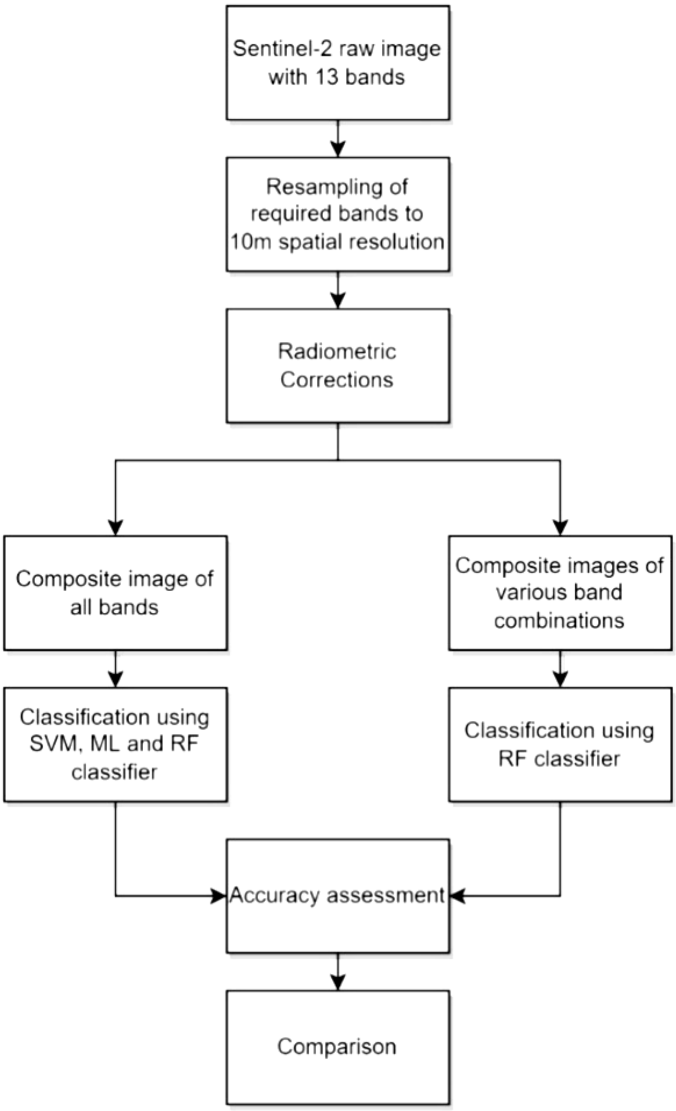

Figure 4: Image Processing Workflow using Sentinel-2 Imagery

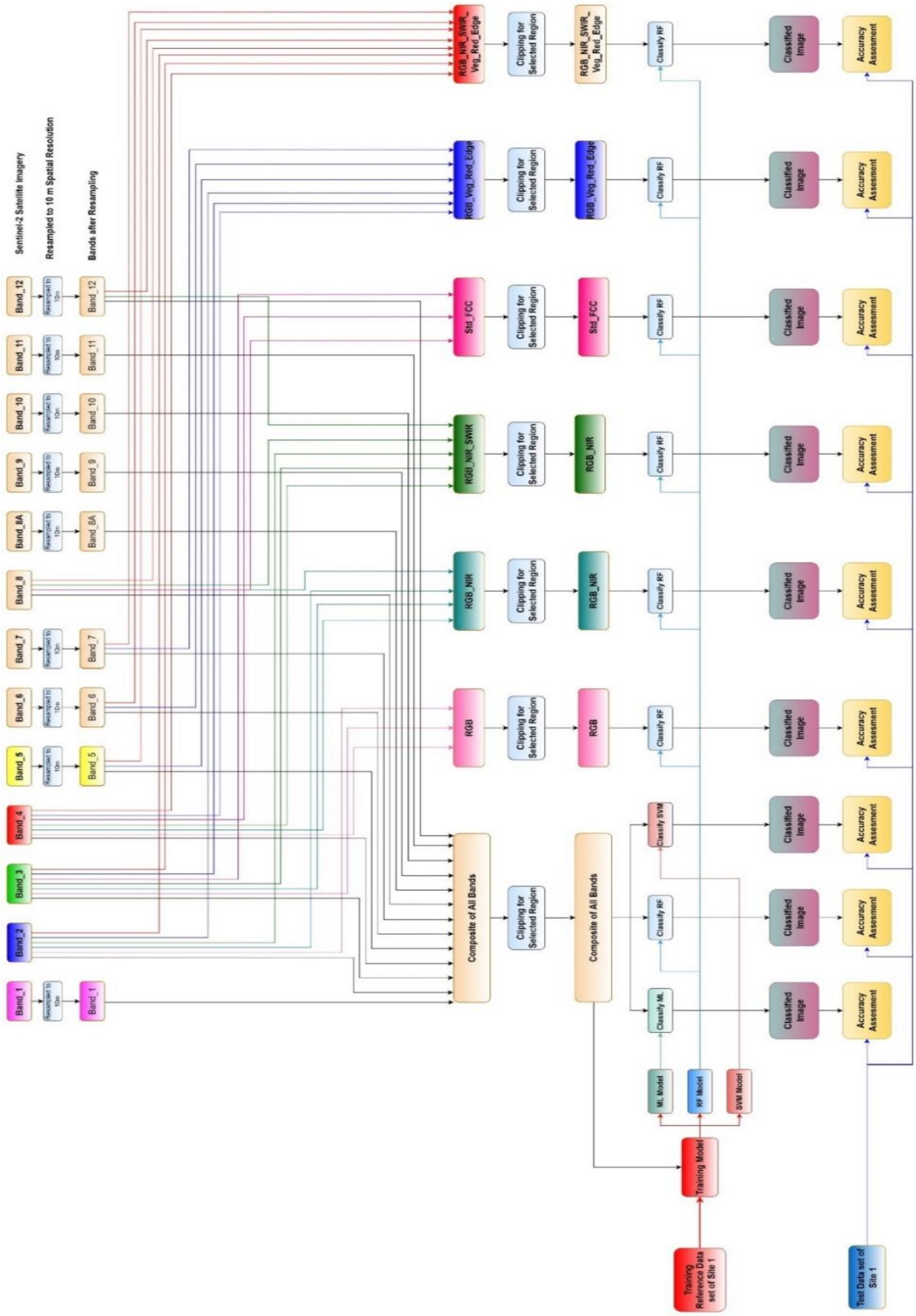

Figure 5: Block Schematic of Image Processing

The intricate image processing steps are illustrated in figure 5. The resampled bands with a high 10m spatial resolution are utilized to create composite images which are subsequently clipped to eliminate any areas outside the scope of the study region. To start, a composite image containing all 13 bands is produced. This composite image is then classified using classical classifiers such as ML, RF and SVM with the aim of determining which one performs better under the given circumstances. RF is chosen as the classifier of choice for the remaining composite images which are generated using various band combinations as outlined in table 5.

In order to incorporate the temporal dimension into the analysis, composite images are generated using the RGB_NIR_SWIR band combinations across multiple dates. Specifically, time series images spanning from 2 to 6 dates are utilized for the multitemporal image processing with the specific dates outlined in table 6.

Table 5
Details of the Composite Images Prepared by Various Band Combinations.

S.N.	Acronyms	Details	Bands
1	RGB	Composite image of Red, Green and Blue bands	S_Band_4, S_Band_3, S_Band_2
2	RGB_NIR	Composite image of Red, Green, Blue and NIR bands	S_Band_4, S_Band_3, S_Band_2, S_Band_8
3	RGB_NIR_SWIR	Composite image of Red, Green, Blue, NIR and SWIR bands	S_Band_4, S_Band_3, S_Band_2, S_Band_8, S_Band_12
4	Std_FCC	Standard False colour composite i.e.,composite image of NIR, Red and Green bands.	S_Band_8, S_Band_4, S_Band_3
5	RGB_Veg_Red_Edge	Composite image of Red, Green, Blue and Veg Red Edge bands	S_Band_4, S_Band_3, S_Band_2, S_Band_5, S_Band_6, S_Band_7
6	RGB_NIR_SWIR_ Veg_Red_Edge	Composite image of Red, Green, Blue, NIR, SWIR and Veg Red Edge bands	S_Band_4, S_Band_3, S_Band_2, S_Band_8, S_Band_12, S_Band_5, S_Band_6, S_Band_7

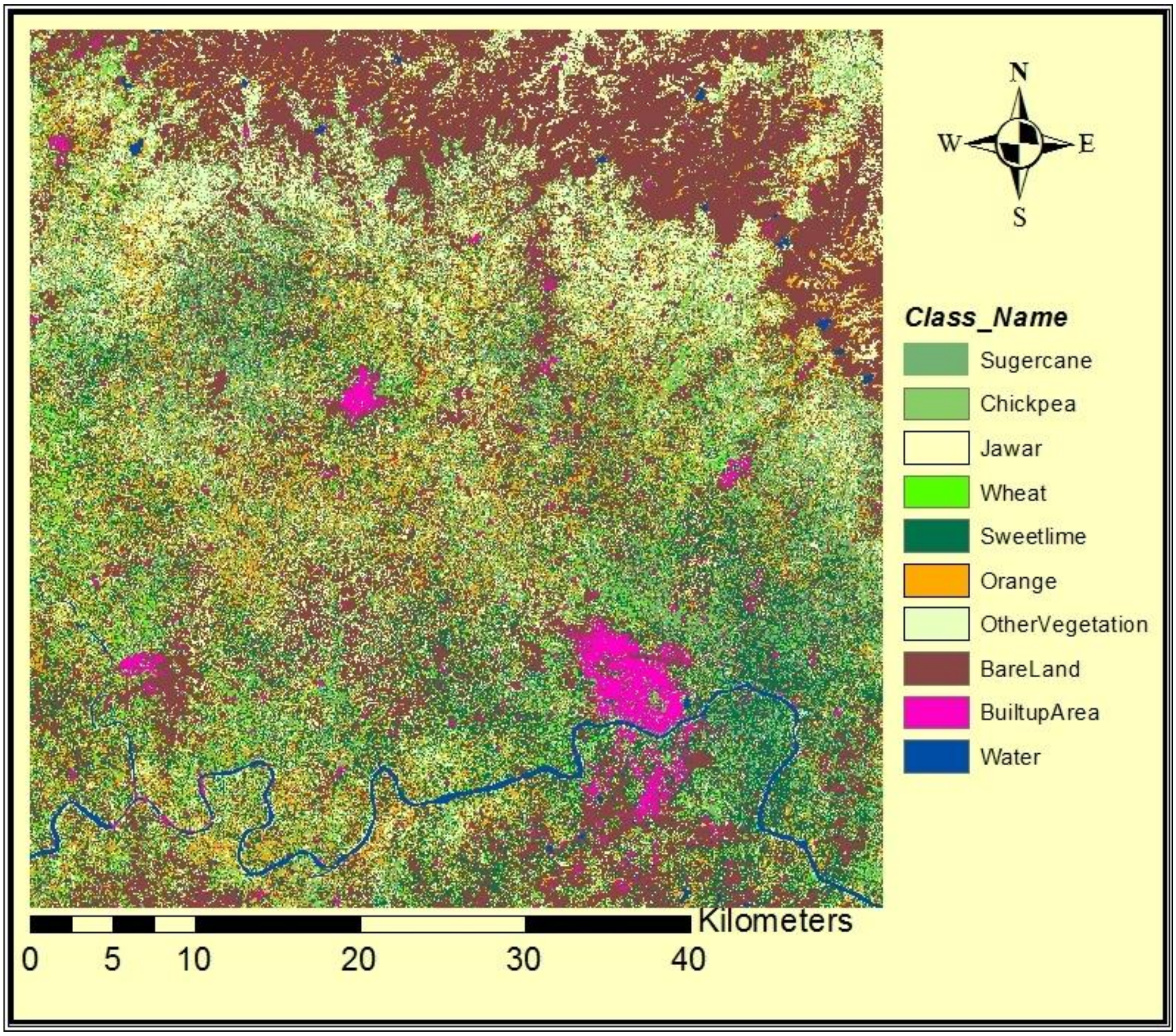

Figure 6: Random Forest Classified Image of 6-Date Multi-Temporal Composite RGB_NIR_SWIR

The composite images obtained from the image processing pipeline are subjected to a classification process using the random forest (RF) algorithm along with reference training data. The accuracy of the classification is then evaluated using a separate test dataset which is essential for performance analysis.

Results and Discussion

Overall accuracy (OA), Producer's Accuracy (PA), User's Accuracy (UA) and Kappa coefficient (k) are matrices used for comparing the accuracy of various classification methods for various combinations of band composite images. In the realm of remote sensing, matrices such as Overall Accuracy (OA), Producer's Accuracy (PA), User's Accuracy (UA) and Kappa coefficient (k) are essential for evaluating the precision of different classification techniques when utilizing various band composite images. The first step is to determine the appropriate classifier suitable for the given classes and imagery.

As demonstrated in table 7, the three classical classifiers (ML, RF, SVM) commonly used in remote sensing are implemented to assess their performance. The RF classifier's Kappa coefficient is relatively superior to the remaining two classifiers for crop cover identification, despite its OA being similar to that of an ML classifier. Thus, the RF classifier is deemed the most significant and utilized as a classification tool for further experimentation.

In the pursuit of achieving greater accuracy, a series of regressive experiments were conducted to analyze minute changes in composite images with various bands of single date satellite data. The results, as presented in table 8, showed a significant improvement in accuracy for both land cover and crop identification upon inclusion of the NIR band with R, G and B bands. The overall accuracy of land cover increased from 81.75% to 86.54% while the crop cover increased from 78.14% to 82.36%. Further improvements were observed with the inclusion of the SWIR band, resulting in an overall accuracy of 87.38% and 82.36% for land cover and crop cover respectively.

A standard false colour composite (Std_FCC) image was also prepared, classified and its accuracy was observed to have reduced to 78.56%. An experiment was carried out using a composite image with the combination of vegetation red edge bands with RGB (RGB_Veg_Red_Edge) but the accuracy was found to be comparatively lower than the RGB_NIR_SWIR combination.

Table 6
Details of Image Acquisition in Various Multi-Temporal Composite Image of RGB_NIR_SWIR Satellite Imagery

Multi-temporal Images	December 2017	January 2018
2 Dates	-	17, 22
3 Dates	-	17, 22, 27
4 Dates	-	7, 17, 22, 27
5 Dates	28	7, 17, 22, 27
6 Dates	18, 28	7, 17, 22, 27

Table 7
Accuracy Analysis Among the Various Classifiers using Composite Image from All 13-Bands of the Pre-Processed Reflectance Imagery of Sentinel-2 Dated 22nd January 2018.

	ML		RF		SVM	
	PA	UA	PA	UA	PA	UA
1. Sugarcane	93.846	87.143	90.769	81.944	70.769	95.833
2. Chickpea	87.5	79.545	70	80	70	59.574
3. Jowar	46.667	87.5	80	75	66.667	55.556
4. Wheat	60	52.174	95	76	75	65.217
5. Sweet Lime	74.667	74.172	72.667	71.711	81.333	72.619
6. Orange	90.222	89.427	92.889	89.126	90.667	91.275
7. Other Vegetation	92.308	74.074	73.846	72.727	95.385	72.941
8. Bare Land	81.429	100	80.714	100	80	99.115
9. Built-Up Area	100	97.345	99.091	100	99.091	100
10. Water	98.846	100	98.846	99.612	98.846	100
OA (Land Cover)	89.278		89.125		88.897	
Kappa (Land Cover)	0.867		0.865		0.863	
OA (Only Crop Cover)	86.087		86.087		85.839	
Kappa (Only Crop Cover)	0.748		0.771		0.74	

Thus, the RGB_NIR_SWIR with vegetation red edge bands was prepared, resulting in an 8-band composite image named RGB_NIR_SWIR_Veg_Red_Edge which was classified with an accuracy of 86.16%. The combination of RGB_NIR_SWIR (5 bands) outperformed all other combinations in the single date imagery with accuracy values of 87.38% and 82.36% and Kappa coefficient values of 0.843 and 0.728 for complete land cover and crop identification respectively. Therefore, for further experimentation using multi-temporal data, the composite of bands RGB_NIR_SWIR is selected as the optimal combination.

In an endeavor to further enhance the accuracy of land and crop identification, a meticulous investigation is conducted by processing date-wise time-series satellite data with the desired band combination. The changes in accuracy and Kappa coefficient for the given classes are presented in table 9 and the details of the dates of image acquisition used for the study are mentioned in table 6. By employing the RGB_NIR_SWIR band combination, the overall accuracy of land cover improves from 87.38% of single date imagery to an impressive 93.69% for the six-date multi-temporal data.

Table 8
Comparison between RF Classified Images with Various Band Combination of Single Date Image of Sentinel-2 Imagery Dated 22nd January 2018.

	RGB		RGB_NIR		RGB_NIR_SWIR		Std_FCC		RGB_Veg_Red_Edge		RGB_NIR_SWIR_VegRedEdge	
	PA	UA	PA	UA	PA	UA	PA	UA	PA	UA	PA	UA
1. Sugarcane	73.87	73.85	70.77	85.19	81.54	79.10	53.85	56.45	72.31	71.21	78.46	75
2. Chickpea	70	66.67	80	61.54	85	66.67	45	52.94	72.5	76.32	77.5	75.61
3. Jowar	53.33	88.89	53.33	88.89	60	90	53.33	88.89	13.33	25	20	75
4. Wheat	55	39.29	85	70.83	80	69.57	75	41.67	75	51.72	85	56.667
5. Sweet Lime	58.67	61.54	72.67	63.01	66.67	63.29	61.33	43.60	70.67	67.09	64.67	64.667
6. Orange	91.79	86.22	90	90.81	91.78	90.97	77.33	87.22	92	87.16	92.22	88.865
7. Other Vegetation	50.77	38.82	67.69	57.14	58.46	59.38	56.92	45.68	64.62	60	61.54	56.338
8. Bare Land	76.43	100	80	98.25	85.71	99.17	82.86	97.48	74.29	96.30	82.14	96.639
9. Built-Up Area	99.09	100	98.18	100	99.09	100	97.27	100	95.46	100	97.27	99.074
10. Water	88.46	92.74	98.85	99.61	98.85	99.61	98.85	100	98.08	98.84	98.85	100
OA (Land Cover)	81.75		86.54		87.38		78.56		85.10		86.16	
Kappa (Land Cover)	0.773		0.833		0.843		0.737		0.814		0.828	
OA (Only Crop Cover)	78.14		82.11		82.36		68.67		81.37		81.242	
Kappa (Only Crop Cover)	0.65		0.711		0.728		0.498		0.69		0.697	

Table 9
Comparison between RF Classified Composite Images of RGB_NIR_SWIR Combination Using Time Series Multi-Temporal Data of Sentinel-2

	2 Dates		3 Dates		4 Dates		5 Dates		6 Dates	
	PA	UA	PA	UA	PA	UA	PA	UA	PA	UA
1. Sugarcane	95.39	81.58	95.39	77.5	96.92	77.78	98.46	73.56	96.92	79.75
2. Chickpea	77.5	73.81	70	82.35	52.5	80.77	57.5	82.14	57.5	82.14
3. Jowar	33.33	71.43	40	85.71	33.33	83.33	60	90	40	100
4. Wheat	95	67.86	95	57.58	95	50	100	80	95	57.58
5. Sweet Lime	80	68.977	81.33	72.62	94.67	88.20	88.67	85.81	92	88.46
6. Orange	89.78	92.45	90.22	92.27	94	97.47	95.33	96.19	96	97.74
7. Other Vegetation	72.31	71.21	70.77	75.41	76.92	70.42	81.54	76.81	81.54	75.71
8. Bare Land	83.57	100	88.57	97.64	90.71	97.69	87.14	98.39	93.57	98.50
9. Built-Up Area	99.09	100	97.27	100	97.27	100	98.18	100	98.18	100
10. Water	99.23	99.61	99.23	100	99.62	99.23	99.62	98.48	99.62	99.62
OA (Land Cover)	89.13		89.58		92.47		92.78		93.69	
Kappa (Land Cover)	0.866		0.871		0.907		0.91		0.922	
OA (Only Crop Cover)	85.47		85.59		89.81		90.81		91.18	
Kappa (Only Crop Cover)	0.769		0.774		0.846		0.855		0.863	

From table 9, it is manifestly apparent that an increase in date-wise data results in an improved overall accuracy and Kappa value for both the complete land cover and crop cover.

Notwithstanding, there are a few noteworthy exceptions to the general trend. It has been observed that certain classes exhibit optimal classification accuracy at different stages of multi-temporal data. For instance, the sugarcane class demonstrates its highest accuracy of 98.46% with 5-date composite satellite data, but this decreases to 96.92% with 6-date satellite imagery.

Conversely, the chickpea class exhibits a decreasing trend in accuracy with the addition of multi-temporal data, declining from 85% (single date) to 57.5% (6 dates). On the other hand, the jowar and wheat classes both exhibit their best accuracy with 5-date imagery at 60% and 100% respectively.

Through empirical investigation, several factors have been examined in this comprehensive experimentation. It has been observed that different classes exhibit varying degrees of improvement or deterioration in accuracy as the time-series satellite data increases. This is due to the changing patterns in the crops as they grow, which affects their discrimination from other classes over time. It has been noted that certain classes contribute to the improvement in accuracy while others contribute to an increase in miss-classification.

In the realm of disaster management, the evaluation of optical multi-spectral satellite data for crop type and land cover identification holds significant potential for mitigating the impact of natural disasters on agriculture. Natural disasters, such as droughts, floods and storms, can cause severe damage to crops and disrupt the agricultural landscape. By utilizing satellite imagery analysis, this research aims to provide critical information on the extent and severity of crop damage caused by such disasters. Accurate identification of crop types and land covers in disaster-affected areas can help authorities assess the magnitude of the crisis, plan response strategies and allocate resources effectively.

Additionally, the use of multi-temporal satellite data enables the monitoring of crop recovery and the evaluation of long-term effects on agricultural landscapes. This information is vital for implementing targeted interventions, facilitating early warning systems and supporting the development of resilient agricultural systems that can better withstand and recover from disasters.

Ultimately, the integration of optical multi-spectral satellite data in disaster management practices can contribute to minimizing the adverse effects of natural disasters on agriculture, ensuring food security and safeguarding the livelihoods of farmers in vulnerable regions like Marathwada, India.

Conclusion

The study investigated the impact of multi-temporal data on land cover and crop classification accuracy using different combinations of spectral bands and classifiers. The results showed that the combination of RGB, NIR and SWIR bands performed the best in both single-date and multi-temporal data, with an overall accuracy of 87.38% for land cover and 82.36% for crop cover. The use of multi-temporal data improved the overall accuracy of land cover classification to 93.69%. However, the accuracy of some classes varied at different stages of multi-temporal data, indicating that the discrimination of changing patterns of crops over time was challenging.

The study highlights the importance of considering the appropriate combination of spectral bands and classifiers in land cover and crop classification. Furthermore, the use of multi-temporal data improves the accuracy of land cover classification. The findings of this study could be useful in land management, resource planning and decision-making, particularly in agriculture and land-use planning. Further research could explore the use of more advanced techniques such as deep learning algorithms in land cover and crop classification.

Our research has shown that random forest outperforms maximum likelihood classifier and support vector machine for crop identification. Standard false colour composite image resulted in less accuracy as compared to other band combinations used in the study. The combination of bands R, G, B, NIR and SWIR gave the best accuracy for both land cover and crop cover identification. However, the results of the crop classes varied with the use of multi-temporal data. Some classes gave better results for single date or two-date imagery while others showed improvement with increased time-series satellite data.

The growth cycle of each class was found to be a contributing factor to this variation. Future studies focusing on the individual class identification using binary classification may provide enhanced results. This research attempted to identify the most appropriate bands for the given classes of land cover, resulting in increased accuracy while reducing computational burden.

The findings of this study have implications for disaster management. By utilizing optical multi-spectral satellite data, accurate and timely information about the extent and impact of disasters on crop types and land cover can be obtained.

This data can assist in assessing damage, identifying vulnerable areas and facilitating targeted relief efforts. The ability to quickly identify changes in land cover and crop patterns using satellite imagery contributes to early warning systems and proactive disaster management strategies. This study highlights the role of optical multi-spectral satellite data in enabling more efficient decision-making to mitigate the impact of disasters on agriculture and land resources.

Acknowledgement

We acknowledge the funding from All India Council for Technical Education (AICTE), New Delhi, India, for this research project. We are thankful to the ESA and USGS for providing satellite imagery for our selected regions and durations.

References

1. Bhuiyan C., Saha A.K., Bandyopadhyay N. and Kogan F.N., Analyzing the impact of thermal stress on vegetation health and agricultural drought–a case study from Gujarat, India, *GIScience & Remote Sensing*, **54,** 678–699 **(2017)**

2. Ferrant Sylvain et al, Detection of irrigated crops from Sentinel-1 and Sentinel-2 data to estimate seasonal groundwater use in South India, *Remote Sensing*, **9**, 1119 **(2017)**

3. Gerald Forkuor, Kangbeni Dimobe, Idriss Serme and Jerome Ebagnerin Tondoh, Landsat-8 vs. Sentinel-2: examining the added value of sentinel-2's red-edge bands to land-use and land-cover mapping in Burkina Faso, *GIScience & Remote Sensing*, **55,** 331–354 **(2018)**

4. Gulati Ashok, Chatterjee Tirtha and Hussain Siraj, Indian Council for Research on International Economic Relations **(2018)**

5. Hanuschak George, Obtaining timely crop area estimates using ground-gathered and LANDSAT data, Dept. of Agriculture, Economics, Statistics and Cooperatives Service **(1979)**

6. Jain Praveen Kumar and Srivastava Pramod Kumar, Indian Government Schemes on Agriculture, *International Journal of Modern Agriculture*, **10(2)**, 2012-2019 **(2021)**

7. Kadam C.M., Kale S.R. , Bhosle U.V. and Holambe R.S., A Machine Learning Approach to Statistical Analysis and Prediction of Rainfall and Drought in the Marathwada Subregion, International Conference on Emerging Smart Computing and Informatics (ESCI), Pune, India, 1-6 **(2023)**

8. Kale S.R. and Holambe R.S., Proposed Methods for Enhancement in Land Use Land Cover (LULC) Identification Using Various Existing and Novel Band Arithmetic Approaches, *Papers in Applied Geography*, **8(2),** 125-145 **(2022)**

9. Kale Shashikant R., Satellite Image Analysis for Agricultural Applications, Shodhganga **(2018)**

10. Kumar Vineet, Kumari Mamta and Saha S.K., Discrimination of basmati and non-basmati rice types using polarimetric target decomposition of temporal SAR data, *Current Science*, **110**, 2166–2169 **(2016)**

11. Kussul N., Lavreniuk M., Skakun S. and Shelestov A., Deep Learning Classification of Land Cover and Crop Types Using Remote Sensing Data, *IEEE Geoscience and Remote Sensing Letters*, **14**, 778-782 **(2017)**

12. Lillesand Thomas, Kiefer R.W. and Chipman Jonathan, Remote sensing and image interpretation, John Wiley & Sons **(2015)**

13. Lozano-Tello Adolfo et al, Crop identification by massive processing of multiannual satellite imagery for EU common agriculture policy subsidy control, *European Journal of Remote Sensing*, **54(1),** https://doi.org/10.1080/22797254.2020.1858723, 1-12 **(2021)**

14. Madhusudhan L., Agriculture role on Indian economy, *Business and Economics Journal*, **6**, 1 **(2015)**

15. Mishra Ashok K. and Singh Vijay P., A review of drought concepts, *Journal of Hydrology*, **391**, 202–216 **(2010)**

16. Ni Rui et al, Effectiveness of Common Preprocessing Methods of Time Series for Monitoring Crop Distribution in Kenya, *Agriculture (Multidisciplinary Digital Publishing Institute)*, **12**, 79 **(2022)**

17. Pandey Akshay and Jain Kamal, An intelligent system for crop identification and classification from UAV images using conjugated dense convolutional neural network, *Computers and Electronics in Agriculture*, **192**, 106543 **(2022)**

18. Pelletier Charlotte, Silvia Valero, Jordi Inglada, Nicolas Champion and Gérard Dedieu, Assessing the robustness of Random Forests to map land cover with high resolution satellite image time series over large areas, *Remote Sensing of Environment*, **187**, 156–168 **(2016)**

19. Reddy Amulya Kumar N., An Indian village agricultural ecosystem- case study of Ungra village, Part II: Discussion, *Biomass*, **1(1)**, 77-88 **(1981)**

20. Singh Jitendra, Devi Umamaheswari, Jagabondhu Hazra and Kalyanaraman Shivkumar, Crop-identification using sentinel-1 and sentinel-2 data for indian region, IGARSS 2018-2018 IEEE International Geoscience and Remote Sensing Symposium, **1**, 5312–5314 **(2018)**

21. Sivakumar M.V.K. and Hinsman Donald E., Satellite Remote Sensing and GIS Applications in Agricultural Meteo-Rology and WMO Satellite Activities, Satellite Remote Sensing and GIS Applications in Agricultural Meteorology, 1-22 **(2003)**

22. Stefani Daryanto, Lixin Wang, Pierre André Jacinthe, Global synthesis of drought effects on cereal, legume, tuber and root crops production: A review, *Agricultural Water Management (Elsevier)*, **179** 18-33 **(2017)**

23. Tian Fuyou, Bingfang Wu, Hongwei Zeng, Xin Zhang and Jiaming Xu, Efficient Identification of Corn Cultivation Area with Multitemporal Synthetic Aperture Radar and Optical Images in the Google Earth Engine Cloud Platform, *Remote Sensing*, **11,** 629 **(2019)**

24. Udmale Parmeshwar, Ichikawa Yutaka, Manandhar Sujata, Ishidaira Hiroshi and Kiem Anthony S., Farmers′ perception of

drought impacts, local adaptation and administrative mitigation measures in Maharashtra State, India, *International Journal of Disaster Risk Reduction,* **10,** 250-269 **(2014)**

25. Yang Chenghai, Everitt James H. and Murden Dale, Evaluating high resolution SPOT 5 satellite imagery for crop identification, *Computers and Electronics in Agriculture,* **75,** 347-354 **(2011)**.

(Received 09th May 2023, accepted 15th July 2023)